Soils and Rocks
An International Journal of Geotechnical and Geoenvironmental Engineering
www.soilsandrocks.com
ISSN 1980-9743
ISSN-e 2675-5475

Influence of intrinsic variability in anthropic slopes

Cristhian Mendoza[1#], Catalina Lozada[2,3]

Article

Keywords
Anthropic slopes
Monte Carlo simulations
Strength reduction method
Variability of geotechnical parameters

Abstract

Anthropic slopes are common in constructing embankments and earth dams and forming open pit mines and fills, among others. However, these slopes artificially built sometimes could fail due to the variability of the soils, lack of expertise in determining the design parameters, and lack of knowledge of the soil's true behavior and construction methods, among others. To address these problems, physical models were made in a geotechnical centrifuge with similar characteristics to study the effect of variability. Subsequently, Monte Carlo simulations were performed using finite element models (FEM) with random geotechnical parameters for an elastic model with Mohr-Coulomb failure criteria. From these simulations, the influence of geotechnical parameters on the factor of safety and deformations was observed. The results show that the coefficient of variation obtained for the factor of safety was less than the coefficient of variation of the geotechnical parameters taken into account. This means that the coefficient of variation of the factor of safety is not the sum or the average of the coefficients of variation taken in the analysis. However, when the factor of safety is more or less constant, but the coefficient of variation of the parameters increases, the probability of failure may increase. This shows that a slope with a factor of safety greater than one can have a high probability of failure. In addition, low friction angle and low cohesion values tend to present more significant slope crest displacements.

1. Introduction

The construction of artificial slopes is a common practice in practical geotechnics. Some examples of uses are in the construction of embankments, earth dams for mining, earth dams, formation of open pit mines, among others. However, these artificially formed slopes sometimes fail. This could be explained by the intrinsic variability of the soils, lack of expertise in determining the design parameters, lack of knowledge of the true behavior of the soil, inadequate design and construction methods, among others. The research presented here studies the influence of the variation of geotechnical parameters on the behavior of the factor of safety (*FS*) on slopes, trying to understand the possible reasons why one slope fails and another does not, if they were both built using similar materials and following the same construction method.

Studies that have contributed to a better understanding of the variability and sensitivity of the probability of failure for a factor of safety are presented by Lacasse & Nadim (2007), Phoon & Kulhawy (1999) and Tan et al. (2003) . Additionally, Phoon et al. (2006) have experimentally shown that performing many tests can reduce the standard deviation, while Gong et al. (2017) have shown that numerical techniques can optimize site investigation and reduce exploration costs to obtain optimal characterizations.

The effect of variability on slopes has become vitally important in recent years (Jiang et al., 2022). The Strength Reduction Method has been commonly implemented in slope stability and is often preferred over the Limit Equilibrium Methods because assumptions regarding inter-slice forces are not required (Dyson & Tolooiyan, 2019). Zienkiewicz et al. (1975) developed one of the first methods of the Strength Reduction Method (SRM), with a reduction of the shear parameters (cohesion and friction angle). So, slope failure occurs when elements with applied shear stresses exceed the material shear strength, causing excessive distortion. Dyson & Tolooiyan (2018) compared different techniques from Strength Reduction, which showed advantages or disadvantages for different proposals in the literature. Regarding variability geotechnical in slopes, Chok et al. (2015) applied the Local Averaging Subdivision (LAS) technique to incorporate spatial correlation in slope stability. This technique generates random field parameters such as soil weight, elastic modulus, friction angle, cohesion, etc. Dyson & Tolooiyan (2019) conducted a probabilistic slope stability analysis using the Random Finite Element Method (RFEM) combined with processes to determine the level of

[#] Corresponding author. E-mail address: cmendozab@unal.edu.co
[1] Universidad Nacional de Colombia Sede Manizales, Departamento de Ingenierá Civil, Manizales, Colombia.
[2] Pontificia Universidad Javeriana, Departamento de Ingenierá Civil, Bogotá, Colombia.
[3] Escuela Colombiana de Ingeniería Julio Garavito, Departamento de Ingeniería Civil y Ambiental, Bogotá, Colombia.

Submitted on February 9, 2023; Final Acceptance on June 5, 2023; Discussion open until November 30, 2023.
https://doi.org/10.28927/SR.2023.001123

similarity between random fields. The study showed the factor of safety's convergence with less finite element simulation when using the Monte Carlo Method.

The above characteristics create the need to better understand the influence of variability on the factor of safety and the contribution of each geotechnical parameter. This problem is addressed by generating physical models with similar characteristics in a geotechnical centrifuge. This was done starting with a slope with an unstable geometry. Subsequently, Monte Carlo simulations were performed using finite element models (FEM) to introduce the influence of the variability of geotechnical parameters on the factor of safety. This variability was introduced by means of random number generation of the geotechnical parameters. Parameters were generated using two different techniques. The first is when the parameters are not correlated because a parameter should not depend on any variable (Cividini et al., 1983; Lei et al., 2017). With this, it was verified that the calculated factor of safety could capture the behavior of the performed physical models. The second, begins with a slope with an *FS* greater than one, and random numbers are generated when the parameters are correlated because they come from the same test. So, variations in a laboratory test can cause variations in all parameters, for example, the influence of measurement in the test, variations between procedures for the same test, human procedural errors, among others. In both cases, the effect of the intrinsic and epistemic variability of the geotechnical parameters is clear. Finally, the influence of the variability in the deformations was observed, which is a primary variable in the analysis of slope stability. All of the above was performed using an elastoplastic constitutive model with a Mohr Coulomb failure criterion.

The results show that the shear parameters are the most important with the constitutive model used for the FS. The coefficient of variation obtained for the FS was around 20%, this value being lower than the average of the COVs (around 32%) of the parameters, which means the coefficient of variation of the FS is not the sum or average of the COVs of the variables taken into account for the analysis. However, when the factor of safety is close to constant, but the coefficient of variation of the parameters is increased, the probability of failure may increase. In addition, low friction angle and low cohesion values tend to present greater displacements. Thus, better performed shear tests lead to a low standard deviation and a lower probability of failure.

2. Materials and methods

The purpose of this study is to determine the effect of variability on artificial slopes. In a first step, physical models were constructed in the geotechnical centrifuge depicted in Figure 1. This centrifuge is a beam type centrifuge with a ratio to the platform of 610 mm and a maximum acceleration of 200 times the Earth's gravity, supporting a maximum load of 12 kg. Physical models were performed with the

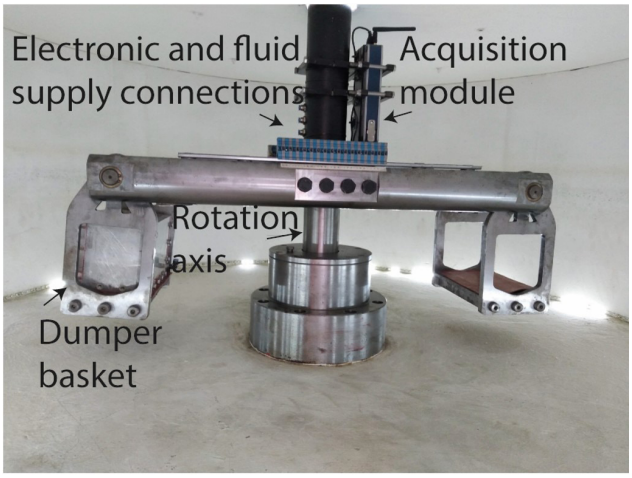

Figure 1. Geotechnical centrifuge at Escuela Colombiana de Ingeniería Julio Garavito.

centrifuge at one hundred times the Earth's gravity (N = 100) for 6 minutes. The failure zones were obtained for each model, analyzing the images before and after the test in the centrifuge. The magnitude of resultant displacements for the models was obtained using the software GeoPIV_RG (White & Take, 2002; Stanier et al., 2016). Then, numerical models in FEM were performed to compute the factor of safety, the position of the failure surface, and resultant displacements. The failure surface depth and resulting displacements as found in physical and numerical models were compared.

2.1 Soil properties

Kaolinite clay, prepared using a slurry state with a water content of 1.5 times the liquid limit, was the soil used in the physical model in the geotechnical centrifuge. Then, oedometric consolidation was performed by doubling the applied load until reaching 30 kPa in the automatic consolidation apparatus shown in Figure 2a. As shown in Figure 2b, a sand layer was added at the bottom of the model to obtain double path drainage to accelerate consolidation. Two models were prepared and consolidated identically to obtain the unitary weight in the nearest soil. The characterization tests, consolidated undrained triaxial tests, and oedometric tests were performed to obtain the main parameters and characteristics of the soil. The results of the tests were: classification by the USCS as a high plasticity silt MH, Liquidity limit of 73.34%, Plasticity limit of 45.48%, Shrinkage limit of 33.28%, Specific Gravity of 2.61, Effective cohesion of 5.5 kPa, Effective friction angle of 24 °, Saturated hydraulic conductivity of 1.7 × 10-5 m/s (from the consolidation curve), and Unitary weight of 14.6 kN/m^3.

2.2 Physical models

Two physical models were tested in the geotechnical centrifuge at an acceleration of one hundred times gravity.

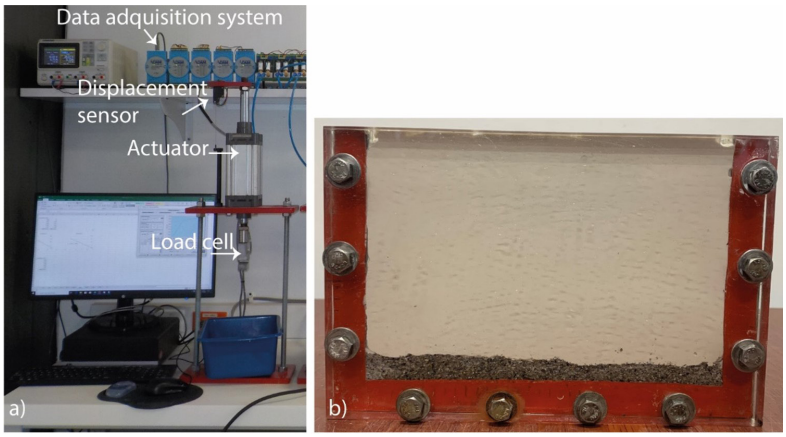

Figure 2. (a) Oedometric consolidometer apparatus for centrifuge models, (b) consolidated soil sample.

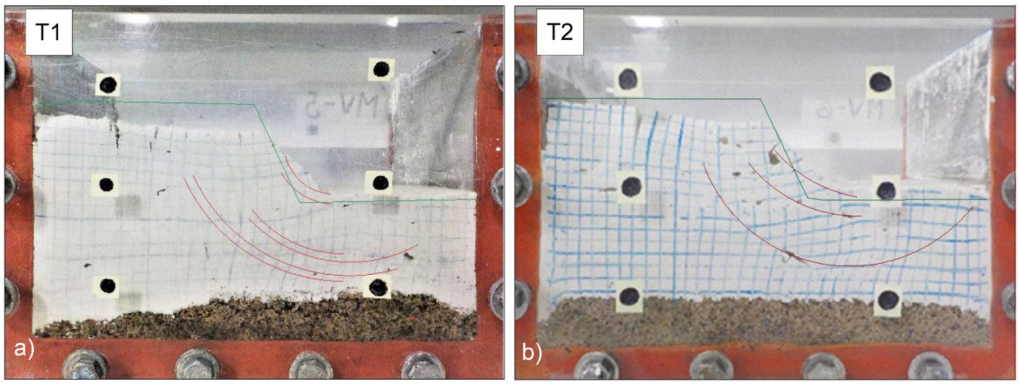

Figure 3. Physical models of slope stability: (a) test T1, (b) test T2.

The models were fabricated with a slope of 67 ° and a height of 3.5 m for the prototype scale. This geometry was obtained by cutting the slope with a wire before the test in the centrifuge (see Figure 2b). The simulated time of the test in the centrifuge for the prototype scale is 42 days. The scaling laws for the centrifuge models at 100 times gravity (N = 100) are shown in Table 1, and the physical models are shown in Figure 3. Multiple sliding surfaces are developed in these models based on Figure 3. In both models, it is observed that the sliding mechanism begins at the toe of the slide, followed by deep sliding failures. An important observation consisted in the differences in the behavior in the displacements for the two models. So, the two models were built in similar conditions, but they presented different failure surfaces. Some of the reasons for these differences include, for example, epistemic variability in the construction of the physical model in consolidation, soil preparation, and soil sample manipulation. These reasons can be extrapolated to the real condition in the field in the construction of artificial slopes.

Table 1. Relevant scaling factors for centrifuge models.

Parameter	Scaling factor	Prototype scale	Model scale
Length H	1/N	7.5 m	7.5 cm
Length B	1/N	4 m	4 cm
Length L	1/N	16 m	16 cm
Time (consolidation)	$1/N^2$	42 days	6 min

3. Implementation of the strength reduction method with randomness

3.1 Constitutive model

The constitutive model used in the present research was elastic with yield criterion of Mohr–Coulomb. The criterion is shown in Equation 1, where the criterion is a function of τ (the shear stress of the soil), c (the cohesion of the soil),

σ_n (the normal stress), and ϕ (the friction angle of the soil). So, Equation 1 shows the increase of shear strength as normal stress increases (or the influence of hydrostatic stress), as shown in Figure 4. In addition, the relationship between stress and strain tensors depends on an elastoplastic tensor (or elastoplastic modulus). This elastoplastic tensor is divided into two-parts. The first part has elastic behavior with the elasticity modulus E and Poisson's ratio μ. The second part works when stress paths reach the yielding criterion in the function of the shearing parameters (c and ϕ).

$$\tau = c + \sigma_n \tan\phi \tag{1}$$

3.2 Strength reduction method (SRM)

To understand slope stability by finite element methods (FEM), the strength reduction finite element method (SRFEM) was implemented in Abaqus 6.21. SRFEM methods have been widely accepted among geotechnical engineers (Dyson & Tolooiyan, 2018). Some advantages of the SRFEM method are that there are no assumptions about the location or shape of the failure surface, similar to the interpretation of the limit state, no assumptions of inter-slice forces, can simulate soils heterogeneously, and show slope displacements. The SRFEM method was presented by Zienkiewicz et al. (1975). Since this work, many other researchers have used the SRFEM method for slope stability, for example, Ugai (1989), Matsui & San (1992), Ugai & Leshchinsky (1995), Dawson et al. (1999), Griffiths & Lane (1999), Yang et al. (2012), Dyson & Tolooiyan (2018), Seyed-Kolbadi et al. (2019) and others. The method consists of adjusting the strength parameters until the slope is unstable. A factor realizes this adjustment, and this factor is the slope factor of safety, as shown below:

$$c = \frac{C_0}{FS} \tag{2}$$

$$\phi = \tan^{-1}\frac{\tan\phi_0}{FS} \tag{3}$$

where c_0 and ϕ_0 are the original cohesion and friction angle provided by soil, and FS is the strength reduction factor to maintain equilibrium. The final strength reduction factor can be obtained in different ways in the function of the definition of slope failure. For example, Dyson & Tolooiyan (2018) showed three criteria. First is the development of plastic zones from the toe to the head of slope. Second is the development of large deformation (defined by the user) in the function of tolerable nodal displacement. The third is the solution non-convergence, often symptomatic of a failure in FEM slope subsidence simulations. Cse (2021) and Tschuchnigg et al. (2015) showed that the successful application of SRM is the criterion for detecting global instability. In general, non-convergence is taken as a criterion for detecting global instability. However, the presence of complicated loads and geometries can prematurely terminate a finite element analysis for nonlinear finite element models. So, non-convergence may not be a suitable criterion for detecting global instability due to numerical or local instabilities.

SRM is not built into the Abaqus program (Dyson & Tolooiyan, 2018). This research used a rule based on the total model plastic dissipated energy ratio to the total model internal strain energy. If this ratio is more significant than 0.2, the model is considered globally unstable. This implementation of SRM is based on the proposal by Cse (2021). It also incorporates the effect of geotechnical variability of parameters for the Monte Carlo method. The automatic calculus of the variability effect into FS slope stability is shown below:

First, it produced an FEM slope model, as shown in Section 3.3.

Second, random parameters were included in FEM simulations, as shown in Section 3.4.

Third, it assumed an interval corresponding from FS stable to FS unstable. Then, iterations were run with reduced cohesion and friction angle to intervals for FS, where FS was the mean value between FS stable and FS unstable. FEM models with reduction parameters were run with a Python script for Abaqus.

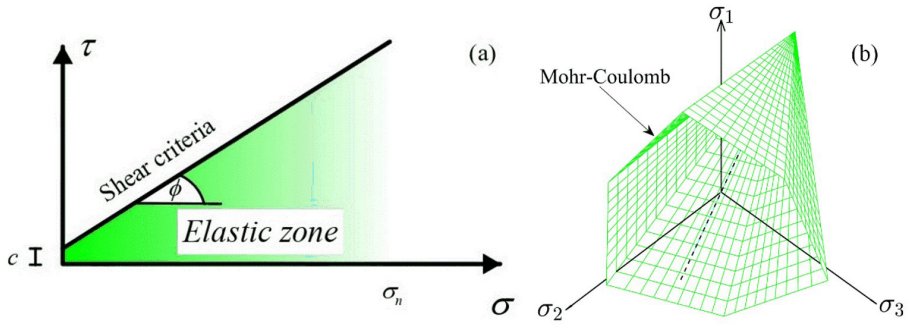

Figure 4. Scheme of the shear criteria to Mohr-Coulomb: (a) *p-q* plane, (b) π-plane [adapted from Helwany (2007)].

Fourth, the global instability criterion was checked. This criterion was a rule based on the ratio of the total plastic dissipated energy of the model to the total internal strain energy of the model, as explained above. It is clear that there are many other criteria to carry out this implementation, including those shown by Tschuchnigg et al. (2015), Dyson & Tolooiyan (2018) and Seyed-Kolbadi et al. (2019).

Fifth, the interval of unstable and stable factor of safety is reduced.

Sixth, the process is performed iteratively until the difference between the unstable and stable factor of safety is less than a specified tolerance ($\Delta FS = 0.01$).

Seventh, the factor of safety obtained from the Monte Carlo simulations are saved in an external file.

On the other hand, implementing the Mohr-Coulomb criterion into the Abaqus program gives rise to the dilation angle, which was not used in this study. The value taken was 0.1.

3.3 FEM models

The ABAQUS version 6.21 was used to generate the finite element model (FEM) of a slope. A two-dimensional model was constructed with plane strain because it presents a good approximation when inside a thick component loaded only in one plane or when an object is constrained in one direction by rigid walls. Thus, the equations only allow the solution in a plane, and the out-of-plane strains are set to zero (Desai & Siriwardane, 1984). Therefore, the plane strain approximation is an excellent approximation to some slopes and centrifuge models, such as those presented in this paper. An FEM model was developed to obtain the factor of safety *FS* and a displacement analyses in the time. The parameterization of the FEM model geometry was a function of the physical model in the centrifuge. The geometry is shown in Figure 3. CPE4P elements were used in the model (plane strain quadrilaterals, two dimensions, four nodes with pore pressure measurement). In addition, the elements concerted near the slope are small in size for a better response as soon as stresses and strains appear. An FEM model was considered saturated and the water table was placed on the ground.

There are two boundary conditions. The first is a fixed condition at the base of the FEM model. This fixed condition does not allow displacements in the x and y directions (See Figure 5). The second involves the lateral rollers in the side edges of the model. This condition does not allow displacements in the x-direction.

Once the geometry of the FEM model is configured, two analyses are performed. The geostatic stresses are induced by the introduction of gravity forces within the FEM model and strength reduction is conducted for *FS*. Another analysis was induced by gravity forces and a simulation of 42 days with consolidation analysis in FEM.

3.4 Create and include random numbers in FEM simulations

To better understand the behavior of artificial slopes, the effect of the variability of the geomechanical properties of the soil was incorporated into the analyses conducted.

This was done through random finite-element analysis using the well-known Monte Carlo method and an elastic model with the yield criterion of Mohr-Coulomb. Random numbers were generated with the statistical parameters shown in Table 2. Mean values of Table 2 were obtained from tests shown in Section 2.1. Statistical values were typical values for fine soils reported by researchers such as Kirby (1991); Phoon & Kulhawy (1999); Griffiths et al. (2005); Papaioannou & Straub (2012); Llano-Serna et al. (2018) and Zevgolis et al. (2018). The influence of variability on soil properties has been published in the past by Lua & Sues (1996); Lump (1970); El-Kadi & Williams (2000); Griffiths & Fenton (2001); Ching et al. (2012); Cai et al. (2017); Al-Bittar et al. (2018); Bolaños & Hurtado (2022), among others. These researchers used normal distributions, lognormal distributions, Monte Carlo analysis, random fields, and other techniques. Thus, the present paper used lognormal distributions to generate each geotechnical parameter for the constitutive model used. Lognormal distributions are

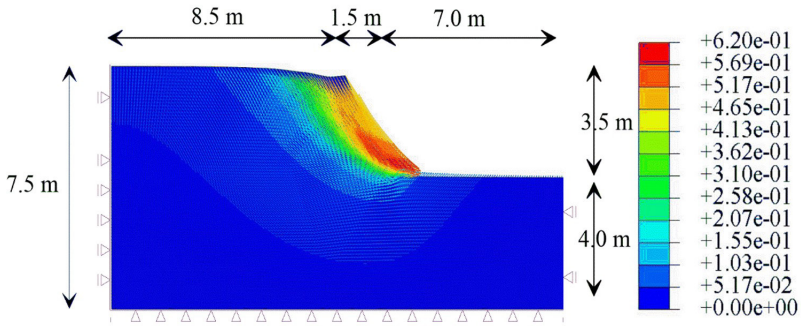

Figure 5. Example of an FEM model for boundary conditions and displacement results in the failure condition.

Table 2. Initial statistical parameters.

Parameter	E	μ	c	ϕ
Unit.	kPa	-	kPa	°
Mean	7500	0.34	5.5	24
Coefficient of variation	0.5	0.15	0.35	0.3
Standard deviation	3750	0.051	1.75	6.9

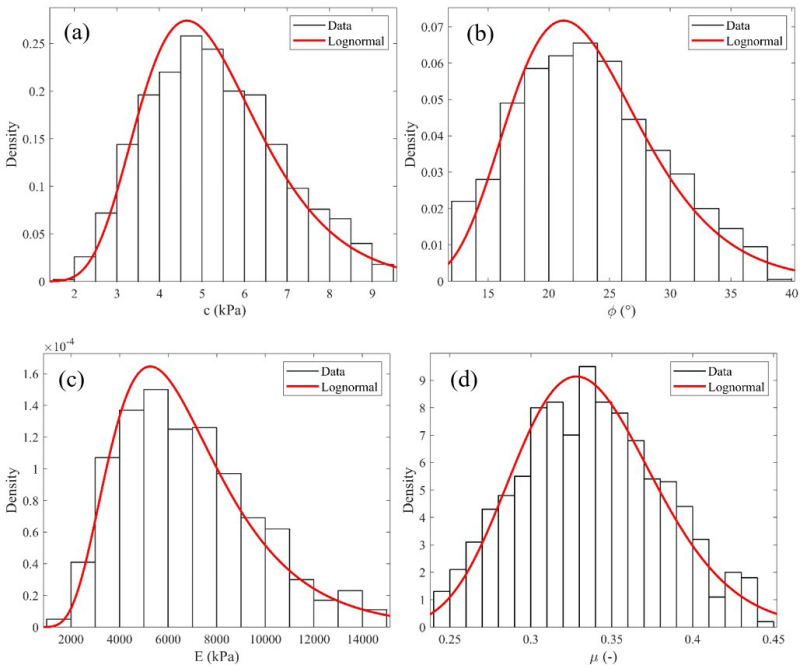

Figure 6. Frequency diagrams and probability distribution function of input variables selected: (a) cohesion, (b) friction angle, (c) elasticity modulus, (d) Poisson's ratio.

well adapted for major geotechnical parameters (Griffiths & Fenton, 2001; Baecher & Christian, 2003).

One thousand random numbers were generated for each geotechnical parameter of the Mohr Coulomb model following a lognormal distribution (see Figure 6). These random parameters were incorporated into the FEM model. The integration was performed by a subroutine in Python and automatically processed because the Abaqus program interacts with Python Script. Subsequently, Monte Carlo simulations were made with geotechnical parameters within an FEM model. This number was used because it stabilized the mean and the standard deviation of *FS*. Then, with the implementation of *FS* shown in Section 3.2, the value of *FS* was obtained for each parameter set used, as shown below in Section 4. Another analysis was the influence of time in displacement for 42 days with transient consolidation. Two analyses were conducted with the same parameter set. Finally, important output variables of the problem FS and displacements were saved in external files. The analyzes in the following sections were based on these external files.

4. Results and discussion

4.1 Displacements fields using PIV

The displacement vectors and the resultant displacements of the physical models were obtained using the Particle Image Velocimetry technique PIV using the GeoPIV_RG software (Stanier et al., 2016). These analyses were performed by comparing two images, the first before the test in the centrifuge and the second after the test in the centrifuge, simulating 42 days for the prototype scale. Figure 7a and 7b show the displacement vectors obtained for all models. This is confirmed when quantifying the displacements obtained in the physical models. The resultant displacements were computed and are shown in Figure 7c and 7d. large displacements were obtained in models with an evident failure mechanism in the slope's body. Indicating lower deformations at greater depths and shifting back movements to the crown of the slope.

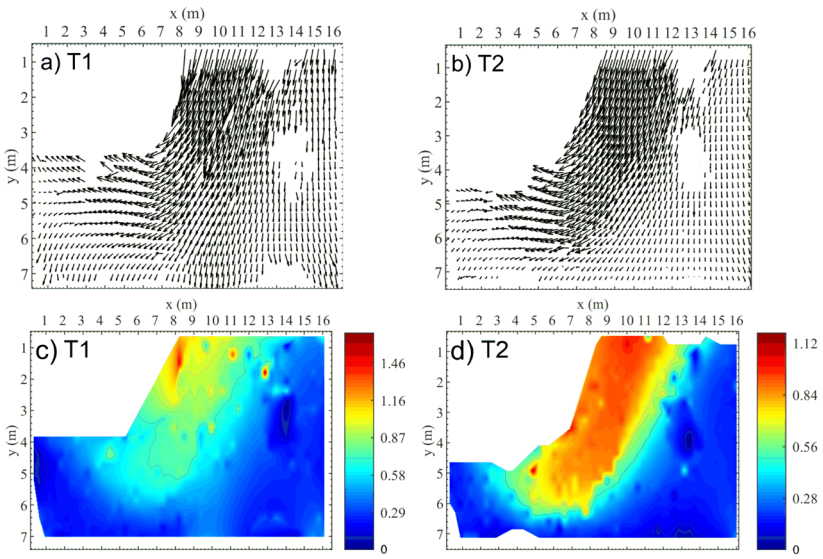

Figure 7. (a) Displacement vectors obtained with GeoPIV_RG of model number one, (b) displacement vectors obtained with GeoPIV_RG of model number two, (c) displacement resultants obtained with GeoPIV_RG of model number one, (d) displacement resultants obtained with GeoPIV_RG of model number two [adapted from Lozada et al. (2022)].

4.2 Main results from random FEM analyses

4.2.1 FS analysis in FEM

The first step was to validate the implementation of the SRM (see Section 3.2). Validation was conducted to compare the implementation of SRM in this study and its implementation in the Plaxis program. The same slope geometry of the physical model (see Section 3.3) was then transferred to Abaqus and Plaxis. However, the initial conditions were changed so that the water table was moved 3 meters below the crest of the slope. The variation of the initial condition was to start with $FS > 1$ because Plaxis does not run to $FS < 1$. It's clear that $FS < 1$ isn't valid (impossible). However, the initial physical model was started from an instability condition (see Figure 2). FS obtained with the implementation of this paper was 1.237 and with Plaxis was 1.221, then the difference between the two was 0.016.

The simulation number for the stabilization of the mean and standard deviation was found based on the validation of the SRM and using the same method proposed by Haldar & Babu (2008), Al-Bittar et al. (2018) and Mendoza & Hurtado (2022) with close to 700 Monte Carlo simulations. The histogram of FS and distributions of cumulative probability of FS were obtained from 1000 simulations, as shown in Figure 8. The statistical values of FS give a mean value of 0.796, a standard deviation of 0.174, and a coefficient of variation of 0.218. In the elastoplastic model with the Mohr-Coulomb rupture criterion, four parameters were varied (E, c, φ, ν) with the coefficient of variations of 0.15 to 0.5 (see Table 2). However, the coefficient of variation of all simulations was 0.218. This value is between the range of COV used. The mean value is less than one, so the results coincide with the experimental tests shown in Figure 2. where the slope used was unstable for this geometric.

All the parameters of the model with the Mohr-Coulomb rupture criterion were varied, E, c, φ, ν with the coefficient of variations from Table 2. So, 700 simulations were conducted, varying each parameter of the model used. This variation was made to show the importance of each parameter in the FS. The important parameters in FS are shown in Figure 9 and compared with variations of all parameters. Figure 9 shows that important parameters for FS are cohesion and friction angle. The other two parameters ν and E don't change the FS value. Table 3 shows the statistical parameters of FS with the variation of cohesion, friction angle, and all parameters, where mean values are similar for cohesion and friction angle. However, COV was lower for cohesion.

The important parameters are from rupture criterion (c and ϕ) for FS. However, these parameters are statistically correlated because they are from the same test. Nevertheless, this study assumes that the parameters cannot be correlated with other parameters or relations because one of the study's goals was to observe the influence of each parameter on FS for slopes. This assumption was made based on Cividini et al. (1983) and Lei et al. (2017) where the parameter definition is a relation (i.e., a model) that describes a certain physical situation using constants. These constants (or parameters) are often introduced to represent the inherent properties of materials. It is clear that there may be a statistical relationship in parameters, but it was not considered in this paper. Some recently published papers about the dependent parameters are by Brinkgreve (2005) and Bolaños & Hurtado (2022).

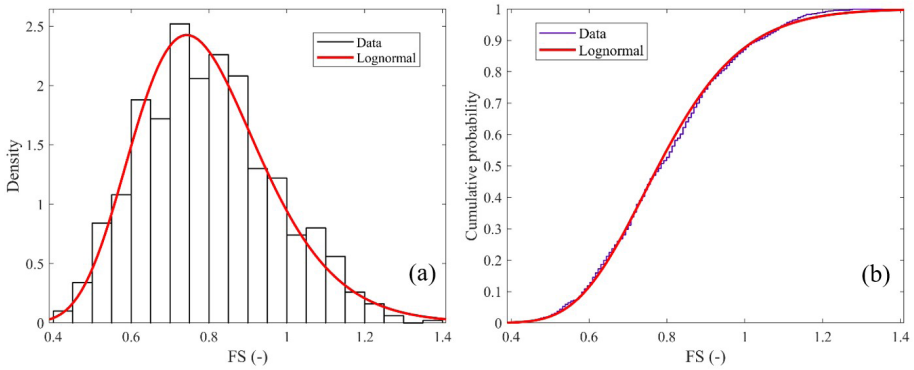

Figure 8. (a) Density curve and histogram of *FS* in the FEM models, (b) distributions of cumulative probability of *FS* in the FEM models.

Table 3. Statistical parameters of *FS* with the variation of cohesion, friction angle, and all parameters.

Parameter	Mean	Standard deviation	Coefficient of variation
c	0.832	0.090	0.108
ϕ	0.840	0.130	0.155
All	0.791	0.166	0.210

Table 4. Statistical parameters of *FS* for each of the combinations from the simulations.

Type	Mean	Standard deviation	Probability of failure (%)
10 c + 10 ϕ	1.230	0.084	0.3148
20 c + 20 ϕ	1.192	0.151	10.0668
30 c + 30 ϕ	1.147	0.202	23.3812
10 c + 20 ϕ	1.209	0.122	4.3224
10 c + 30 ϕ	1.182	0.162	13.0931
20 c + 10 ϕ	1.216	0.123	4.0399
20 c + 30 ϕ	1.168	0.179	17.2956
30 c + 10 ϕ	1.189	0.159	11.8157
30 c + 20 ϕ	1.170	0.146	12.2101

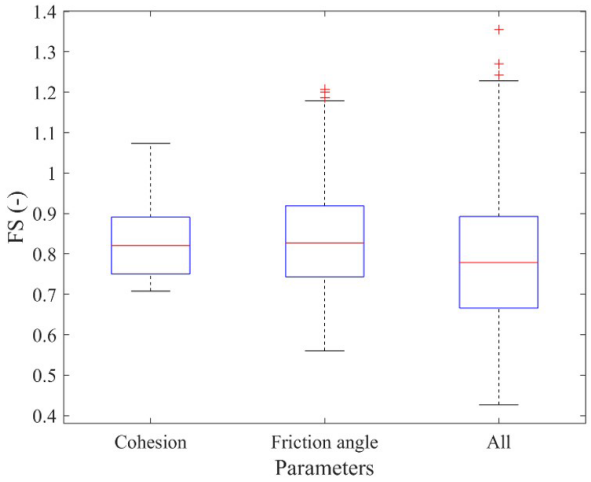

Figure 9. Box-and-whisker plots to *FS* with cohesion, friction angle, and all parameters.

Figure 9 highlights that cohesion and friction angle are important parameters. In addition, the simulations shown in Figure 8 stabilize a mean and a standard deviation of the *FS* near 500 simulations. The cohesion was changed to 11.0 kPa for an FS near 1.2. Then, 500 random numbers were created for cohesion and friction angle parameters. These parameters were built with a COV of 10%, 20%, and 30% to see the influence of the parameters on FS and the probability of failure P_f. Subsequently, the parameters generated with different COVs were combined as follows: 10% cohesion and 10% friction angle, 20% cohesion and 20% friction angle, 30% cohesion and 30% friction angle, 10% cohesion and 20% friction angle, 10% cohesion and 30% friction angle, 20% cohesion and 10% friction angle, 20% cohesion and 30% friction angle, 30% cohesion and 10% friction angle, 30% cohesion and 20% friction angle. In total, 4500 simulations were made. Table 4 shows the main results of the simulations (μ, σ, and P_f).

Figure 10 shows the analysis histograms with equal COVs of 30%, 20%, and 10%. In addition, the curves of a normal distribution are placed. This figure showed that low COVs lead to low standard deviations and almost constant values of *FS*. Then, good characterization tests with calibrated equipment, standardized procedures, and the same measurement systems should lead to low COVs. Also, a standardized construction process is an important factor in reducing standard deviation. These processes lead to a lower probability of failure, as shown in Table 4.

The results from Table 4 are plotted in Figure 11, which shows that the *FS* changes little with the change of the COV. Standard deviation increases as COV increases and mainly with the increase of the COV of cohesion. Thus, a slope with

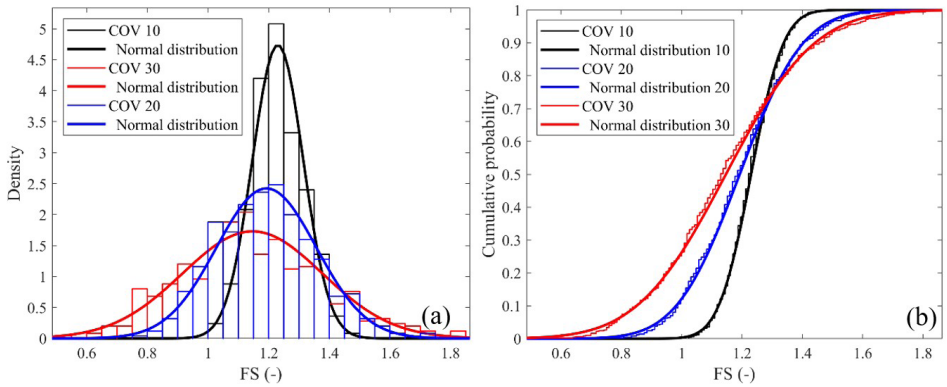

Figure 10. (a) Density curve and histogram of FS for different COVs, (b) distributions of cumulative probability of FS for different COVs.

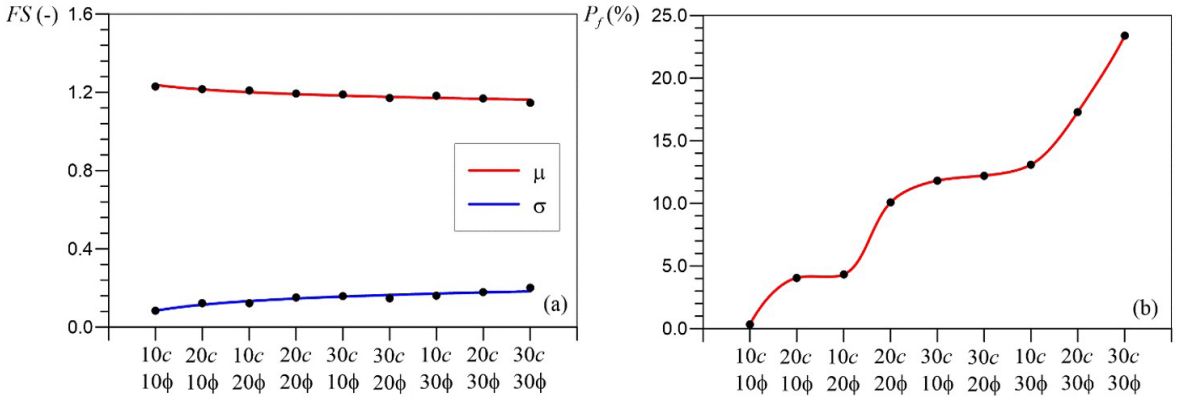

Figure 11. (a) Mean and standard deviation of FS from the simulations for the cases studied, (b) probability of failure for the cases studied.

a nearly constant *FS* can have a higher P_f depending on the increase in the standard deviation of the shear parameters. Nadim & Lacasse (1999) and Lacasse & Nadim (2007) showed that a geotechnical project could have a higher *FS* and a higher probability of failure than a project with a lower *FS* and P_f. Similar results are found in this study. So, a construction process with homogeneous materials and standardized tests can lower the standard deviation, thus lowering the P_f with a constant *FS*. Also, the *FS* methodology does not always guarantee a low probability of failure.

4.2.2 Displacement analysis

A simulated strain analysis for forty-six days was performed as in the simulation in the geotechnical centrifuge. However, the most significant deformation occurred in a few days due to the limitations of the model used, more information can be reviewed in the studies by Soga et al. (2016) and Augarde et al. (2021). This analysis is carried out due to the importance of soil mass displacements in the neighboring structures. Thus, depending on the deformations, the failure of the slope at a certain site may or may not be important. Limit-state models cannot capture this important part of a failure analysis. Figure 12 shows the deformations at the crest of the slope obtained from the Monte Carlo simulations. Figure 12b shows that most deformations are less than 0.2 m. However, depending on the parameters, the displacements of the crest can reach up to two meters. Figure 12c shows that slopes with low friction angle and low cohesion tend to have higher displacements. Regarding the modulus of elasticity, it showed a tendency when there are higher values of the friction angle where there are lower displacements with higher moduli (Figure 12d). However, the displacements presented are not greater than those shown in Figure 12c with respect to low cohesion. In addition, Figure 12c and 12d compare the displacements obtained from the simulations with the displacements obtained from the geotechnical centrifuge tests. This comparison shows that the displacements obtained with the simulations can be similar to those obtained in the centrifuge tests for values close to the parameters obtained experimentally (see Table 2). These results are valid only for the geometry and parameters used in the present research. Furthermore, it is assumed that large crest displacements may indicate large soil mass

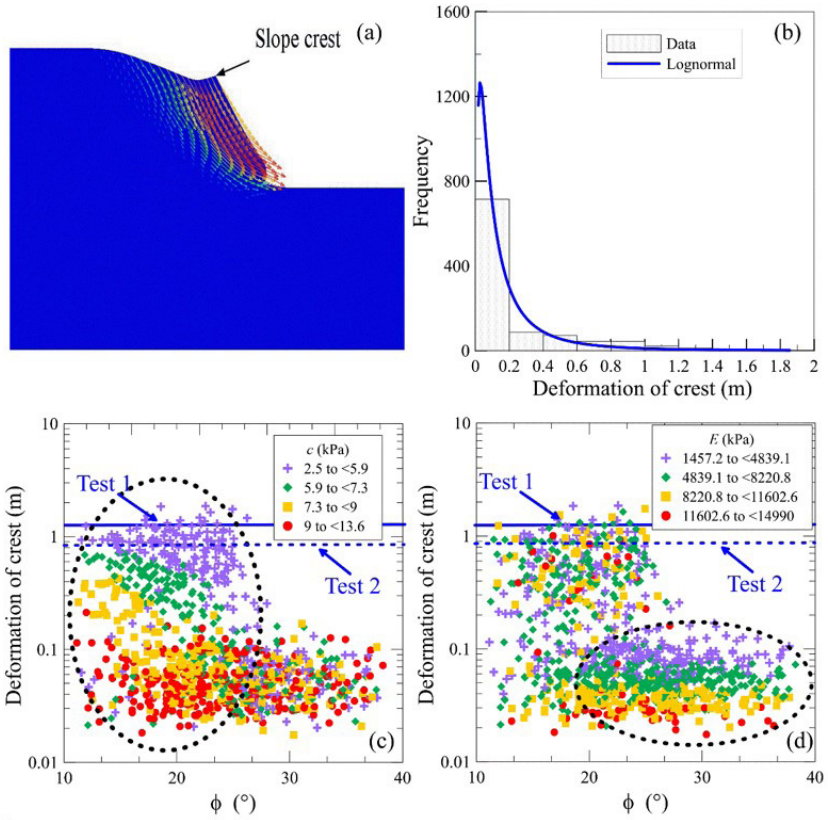

Figure 12. (a) Deformation vectors around of slope, (b) density curve and histogram of crest deformation, (c) and (d) deformation of crest versus variability of parameters.

displacements. A contribution of the present research is that in soil with a low friction angle, it would be essential to know the cohesion value, even if it is low. Therefore, this parameter should be characterized in the best possible way to lower the standard deviation (Phoon et al., 2006).

5. Conclusions

This study presents an innovative procedure to obtain the impact of the geotechnical parameters in the factor of safety and deformation by considering the natural variability of the soil and the variability resulting from the quality of the tests. The following conclusions can be drawn:

- The results of simulations show that the value of the factor of safety is nearly constant with the change of COV in the geotechnical parameters. Standard deviation increases with COV and mainly with the increase of the COV of cohesion. Thus, a slope with a nearly constant *FS* can have a higher P_f depending on the increase in the standard deviation of the shear parameters. Thus, a slope could have a higher *FS* and a higher probability of failure than a similar slope with a lower *FS* and P_f. An *FS* methodology does not always guarantee a low probability of failure. An alternative can be a good characterization of the materials and a standardized construction process to lower the standard deviation, thus reducing the P_f.
- All parameters of the elastoplastic model with the Mohr-Coulomb rupture criterion were varied. The crucial parameters in *FS* are cohesion and friction angle. Displacements of the crest show that slopes with low friction angle and low cohesion tend to present greater displacements. The modulus shows a trend when friction angles are high, but displacements are low.
- The displacements by the FEM simulations are within the limits of the displacements obtained from the geotechnical centrifuge tests. Also, FEM simulations can capture slope stability (factor of safety) in centrifuge tests of slopes. Thus, FEM simulations are a good method to capture the behavior of slopes with the variability of geotechnical parameters.

Acknowledgements

The authors express their gratitude to Universidad Nacional de Colombia, Pontificia Universidad Javeriana and Escuela Colombiana de Ingeniería Julio Garavito in Colombia for their technical and financial support to this paper.

Declaration of interest

The authors have no conflicts of interest to declare. All co-authors have observed and affirmed the contents of the paper and there is no financial interest to report.

Authors' contributions

Cristhian Mendoza: conceptualization, data curation, visualization, writing – original draft. Catalina Lozada: conceptualization, data curation, methodology, supervision, validation, writing – original draft.

Data availability

The datasets produced and analyzed during the present study are available from the corresponding author upon reasonable request.

List of symbols

c	cohesion of the soil
B	width of the models
COV	coefficient of variation
E	elasticity modulus
FEM	finite element models
FS	factor of safety
H	Height of the models
L	Length of the models
LAS	local averaging subdivision
N	length scale in centrifugal model.
P_f	probability of failure
PIV	particle image velocimetry technique
RFEM	random finite element method
SRFEM	strength reduction finite element method
SRM	strength reduction method
μ	Poisson's ratio
σ_n	normal stress
τ	shear stress of the soil
ϕ	friction angle of the soil

References

Al-Bittar, T., Soubra, A.H., & Thajeel, J. (2018). Kriging-based reliability analysis of strip footings resting on spatially varying soils. *Journal of Geotechnical and Geoenvironmental Engineering*, 144(10), 04018071..

Augarde, C.E., Lee, S.J., & Loukidis, D. (2021). Numerical modelling of large deformation problems in geotechnical engineering: a state of-the-art review. *Soils and Foundations*, 61(6), 1718-1735.

Baecher, G., & Christian, J. (2003). *Reliability and statistics in geotechnical engineering*. John Wiley & Sons.

Bolaños, C.C.M., & Hurtado, J.E. (2022). Effects of soil test variability in the bearing capacity of shallow foundations. *Transportation Infrastructure Geotechnology*, 9, 854-873.

Brinkgreve, R.B. (2005). Selection of soil models and parameters for geotechnical engineering application. In J.A. Yamamuro & V.N. Kaliakin (Eds.), *Soil constitutive models: evaluation, selection, and calibration* (pp 69-98). ASCE.

Cai, J.S., Yan, E.C., Yeh, T.C.J., Zha, Y.Y., Liang, Y., Huang, S.Y., Wang, W.K., & Wen, J.C. (2017). Effect of spatial variability of shear strength on reliability of infinite slopes using analytical approach. *Computers and Geotechnics*, 81, 77-86..

Ching, J., Chen, J., Yeh, J., & Phoon, K. (2012). Updating uncertainties in friction angles of clean sands. *Journal of Geotechnical and Geoenvironmental Engineering*, 138(2), 217-229..

Chok, Y.H., Jaksa, M.B., Griffths, D.V., Fenton, G.A., & Kaggwa, W.S. (2015). Probabilistic analysis of a spatially variable c′-φ′ slope. *Australian Geomechanics Journal*, 50, 17-27.

Cividini, A., Maier, G., & Nappi, A. (1983). Parameter estimation of a static geotechnical model using a Bayes' approach. *International Journal of Rock Mechanics and Mining Sciences & Geomechanics Abstracts*, 20(5), 215-226.

Cse, J. (2021). *Fundamentals of geomechanical and geotechnical finite element modeling using Abaqus and Python*. Independently Published.

Dawson, E., Roth, W., & Drescher, A. (1999). Slope stability analysis by strength reduction. *Geotechnique*, 49(6), 835-840.

Desai, C.S., & Siriwardane, H.J. (1984). *Constitutive laws for engineering materials with emphasis on geologic materials*. Prentice-Hall.

Dyson, A.P., & Tolooiyan, A. (2018). Optimisation of strength reduction finite element method codes for slope stability analysis. *Innovative Infrastructure Solutions*, 3, 38. http://dx.doi.org/10.1007/s41062-018-0148-1.

Dyson, A.P., & Tolooiyan, A. (2019). Prediction and classification for finite element slope stability analysis by random field comparison. *Computers and Geotechnics*, 109, 117-129.

El-Kadi, A.I., & Williams, S.A. (2000). Generating two-dimensional fields of autocorrelated, normally distributed parameters by the matrix decomposition technique. *Ground Water*, 38(4), 530-532..

Gong, W., Tien, Y., Juang, C.H., Martin II, J.R., & Luo, Z. (2017). Optimization of site investigation program for improved statistical characterization of geotechnical property based on random field theory. *Bulletin of Engineering Geology and the Environment*, 76, 1021-1035.

Griffiths, D.V., & Fenton, G.A. (2001). Bearing capacity of spatially random soil: the undrained clay Prandtl problem revisited. *Geotechnique*, 51(4), 351-359..

Griffiths, D.V., & Lane, P.A. (1999). Slope stability analysis by finite elements. *Geotechnique*, 49(3), 387-403.

Griffiths, D.V., Fenton, G.A., & Tveten, D.E. (2005). Probabilistic earth pressure analysis by the random finite element method. In G. Barla & M. Barla (Eds.), *Proc. 11th Int. Conf. on Computer Methods and Advances in Geomechanics (IACMAG 05)*, (Vol. 4, pp. 235–249). Bologna: Pátron Editore.

Haldar, S., & Babu, G.S. (2008). Effect of soil spatial variability on the response of laterally loaded pile in undrained clay. *Computers and Geotechnics*, 35(4), 537-547.

Helwany, S. (2007). *Applied soil mechanics with ABAQUS applications* (1st ed.). Wiley.

Jiang, S.H., Huang, J., Griffiths, D.V., & Deng, Z.P. (2022). Advances in reliability and risk analyses of slopes in spatially variable soils: a state-of-the-art review. *Computers and Geotechnics*, 141, 104498.

Kirby, J.M. (1991). Critical-state soil mechanics parameters and their variation for Vertisols in eastern Australia. *Journal of Soil Science*, 42(3), 487-499.

Lacasse, S., & Nadim, F. (2007). Probabilistic geotechnical analyses for offshore facilities. *Georisk*, 1(1), 21-42.

Lei, B., Xu, G., Feng, M., Zou, Y., Van der Heijden, F., Ridder, D.D., & Tax, D.M. (2017). *Classification, parameter estimation and state estimation: an engineering approach using MAT-LAB*. John Wiley & Sons.

Llano-Serna, M.A., Farias, M.M., Pedroso, D.M., Williams, D.J., & Sheng, D. (2018). An assessment of statistically based relationships between critical state parameters. *Geotechnique*, 68(6), 556-560.

Lozada, C., Mendoza, C., & Amortegui, J.V. (2022). Physical and numerical modeling of clayey slopes reinforced with roots. *International Journal of Civil Engineering*, 20, 1115-1128.

Lua, Y.J., & Sues, R.H. (1996). Probabilistic finite-element analysis of airfield pavements. *Transportation Research Record: Journal of the Transportation Research Board*, 1540(1), 29-38.

Lump, P. (1970). The Safety factors and the probability distributions of soil strength. *Canadian Geotechnical Journal*, 7(3), 225-242.

Matsui, T., & San, K.C. (1992). Finite element slope stability analysis by shear strength reduction technique. *Soils and Foundations*, 32, 59-70.

Mendoza, C., & Hurtado, J.E. (2022). The importance of geotechnical random variability in the elastoplastic stress–strain behavior of shallow foundations considering the geological history. *Geotechnical and Geological Engineering*, 40, 3799-3818.

Nadim, F., & Lacasse, S. (May 14, 1999). Probabilistic slope stability evaluation. In Geotechnical division, Hong Kong Institution of Engineers (Ed.), *Proceedings of the 18th Annual Seminar on Geotechnical Risk Management* (pp. 177-186). Hong Kong: Hong Kong Institution of Engineers.

Papaioannou, I., & Straub, D. (2012). Reliability updating in geotechnical engineering including spatial variability of soil. *Computers and Geotechnics*, 42, 44-51.

Phoon, K., & Kulhawy, F.H. (1999). Evaluation of geotechnical property variability. *Canadian Geotechnical Journal*, 36(4), 625-639.

Phoon, K., Nadim, F., Uzielli, M., & Lacasse, S. (2006). Soil variability analysis for geotechnical practice. *Characterisation and Engineering Properties of Natural Soils*, 3, 1653-1752.

Seyed-Kolbadi, S.M., Sadoghi-Yazdi, J., & Hariri-Ardebili, M.A. (2019). An improved strength reduction-based slope stability analysis. *Geosciences*, 9(1), 55. http://dx.doi.org/10.3390/geosciences9010055.

Soga, K., Alonso, E., Yerro, A., Kumar, K., & Bandara, S. (2016). Trends in large-deformation analysis of landslide mass movements with particular emphasis on the material point method. *Geotechnique*, 66(3), 248-273.

Stanier, S.A., Blaber, J., Take, W.A., & White, D.J. (2016). Improved image-based deformation measurement for geotechnical applications. *Canadian Geotechnical Journal*, 53, 727-739. http://dx.doi.org/10.1139/cgj-2015-0253.

Tan, T.S., Phoon, K.K., Hight, D.W., & Leroueil, S. (2003). *Characterisation and engineering properties of natural soils*. A.A. Balkema.

Tschuchnigg, F., Schweiger, H.F., & Sloan, S.W. (2015). Slope stability analysis by means of finite element limit analysis and finite element strength reduction techniques. Part I: numerical studies considering non-associated plasticity. *Computers and Geotechnics*, 70, 169-177.

Ugai, K. (1989). A method of calculation of total safety factor of slope by elasto-plastic FEM. *Soils and Foundations*, 29(2), 190-195.

Ugai, K., & Leshchinsky, D. (1995). Three-dimensional limit equilibrium and finite element analyses: a comparison of results. *Soils and Foundations*, 35(4), 1-7.

White, D.J., & Take, W.A. (2002). *GeoPIV: Particle Image Velocimetry (PIV) software for use in geotechnical testing*. University of Cambridge.

Yang, X., Yang, G., & Yu, T. (2012). Comparison of strength reduction method for slope stability analysis based on ABAQUS FEM and FLAC3D FDM. *Applied Mechanics and Materials*, 170-173, 918-922.

Zevgolis, I.E., Koukouzas, N.C., Roumpos, C., Deliveris, A.V., & Marshall, A.M. (2018) Evaluation of geotechnical property variability: the case of spoil material from surface lignite mines. In: *5th international civil protection conference—SafeKozani 2018*, Kozani, Greece: SafeGreece.

Zienkiewicz, O.C., Humpheson, C., & Lewis, R.W. (1975). Associated and non-associated visco-plasticity and plasticity in soil mechanics. *Geotechnique*, 25, 671-689.